Delta ribozyme has the ability to cleave *in trans* an mRNA

Guylaine Roy, Sirinart Ananvoranich and Jean-Pierre Perreault*

Département de Biochimie, Faculté de Médecine, Université de Sherbrooke, Sherbrooke, Québec J1H 5N4, Canada

ABSTRACT

We report here the first demonstration of the cleavage of an mRNA *in trans* by delta ribozyme derived from the antigenomic version of the human hepatitis delta virus (HDV). We characterized potential delta ribozyme cleavage sites within HDV mRNA sequence (i.e. C/UGN_6), using oligonucleotide binding shift assays and ribonuclease H hydrolysis. Ribozymes were synthesized based on the structural data and then tested for their ability to cleave the mRNA. Of the nine ribozymes examined, three specifically cleaved a derivative HDV mRNA. All three active ribozymes gave consistent indications that they cleaved single-stranded regions. Kinetic characterization of the ability of ribozymes to cleave both the full-length mRNA and either wild-type or mutant small model substrate suggests: (i) delta ribozyme has turnovers, that is to say, several mRNA molecules can be successively cleaved by one ribozyme molecule; and (ii) the substrate specificity of delta ribozyme cleavage is not restricted to C/UGN_6. Specifically, substrates with a higher guanosine residue content upstream of the cleavage site (i.e. positions –4 to –2) were always cleaved more efficiently than wild-type substrate. This work shows that delta ribozyme constitutes a potential catalytic RNA for further gene-inactivation therapy.

INTRODUCTION

The hepatitis delta virus (HDV), like some viroids and plant viroid-like satellite RNAs, uses self-catalytic RNA sequences to cleave the multimeric strands produced during replication into monomers (for review see ref. 1). Minimal delta self-cleavage RNA strands of both polarities can be separated into two molecules in order to develop *trans* systems which include a delta ribozyme that catalyzes successive cleavage of several molecules of substrate (for reviews see refs 2,3). Delta ribozyme is unique in its natural ability to function in human cells. The ability of ribozymes to specifically recognize a substrate, and subsequently catalyze their cleavage, makes them attractive therapeutic tools for the inactivation of both viral RNA and mRNA associated with human diseases. Delta self-catalytic RNA strands have been shown to be useful for the self-cleavage in cells required to release

a hammerhead ribozyme which subsequently acted *in trans* on a herpes simplex virus mRNA, as well as for the synthesis of RNAs with precise termini required in the production of defective interfering particles of vesicular stomatitis virus (4,5). However, to our knowledge the use of delta ribozyme to cleave an mRNA *in trans* has not been reported. According to the pseudoknot secondary structure proposed for the delta ribozyme, substrate recognition (i.e. specificity) is based on the formation of the P1 stem which includes one G-U wobble basepair followed by six non-specific Watson–Crick basepairs (Fig. 1; ref. 2). Since it has been shown that a pyrimidine (Y) immediately adjacent to the cleavage site is preferable (6), the logical design of a delta ribozyme against any RNA substrate is one containing the stretch YGN_6 as its recognition sequence.

The HDV RNA genome produces a unique mRNA (~0.7 kb) that encodes the two isoforms of the delta antigen (HDAg), the small-HDAg (S-HDAg; 195 amino acids) and the large-HDAg (L-HDAg; 214 amino acids) (1). Both isoforms have crucial roles in the HDV life cycle: S-HDAg is involved in HDV replication, while L-HDAg is required for viral packaging. Consequently, depletion of HDAg mRNA is an ideal means of controlling HDV propagation. The goal of the present work is to investigate the potential of the delta ribozyme in the *trans* cleavage of an mRNA, specifically a derivative of the HDAg mRNA. We report the identification of potential cleavage sites for delta ribozyme on this mRNA by oligonucleotide probing, the production of appropriate ribozymes and their characterization with respect to their ability to cleave both an mRNA and minimal model substrates. The results show that delta ribozyme constitutes a potential catalytic RNA for further gene-inactivation therapy.

MATERIALS AND METHODS

Selection of target sites

All mRNA sequences available in January 1997 from the public database of viroid and viroid-like RNAs were retrieved (http://www.callisto.si.usherb.ca/~jpperra ; 7) and aligned using the ClustalW package (version 1.6; ref. 8). Potential target sites (i.e. those including the sequence YGN_6 and conserved in >80% of the variants) were identified (Table 1).

Plasmids encoding the HDAg mRNA and delta ribozymes

The pKSAgS plasmid carries the S-HDAg mRNA in pBluescript KS+ (Stratagene). Briefly, the S-HDAg mRNA insert [positions 900–1679 of the vHDV.5 variant (according to ref. 7) were retrieved by PCR amplification using pSVL(AgS) (generously provided by Dr John Taylor; ref. 9)] as template. The oligo-nucleotides used in this PCR had restriction sites situated at their 5′ ends so as to facilitate subsequent cloning: HDV1679.66, 5′-CC<u>GGATCCC</u>TCGGGCTCGGGCG-3′ (underlined is the *Bam*HI restriction site); and HDV900.914, 5′-CC<u>AAGCTTC</u>-GAAGAGGAAAGAAG-3′ (underlined is the *Hin*dIII restriction site). Plasmid DNA [pSVL(AgS), 50 ng], 0.4 mM of each oligonucleotide, 200 mM dNTPs, 1.25 mM MgCl$_2$, 10 mM Tris–HCl pH 8.3, 50 mM KCl and 1 U *Taq* DNA polymerase were mixed together in a final volume of 100 μl. We performed one low stringency PCR cycle (94°C for 5 min, 53°C for 30 s, 72°C for 1 min), followed by 35 cycles at higher stringency (94°C for 1 min, 62°C for 30 s, 72°C for 1 min). The mixture was fractionated by electrophoresis in a 1% agarose gel in 1× TBE buffer (90 mM Tris-borate, 2 mM EDTA pH 8.0), the expected band excised and eluted using the QIAquick gel extraction kit (Qiagen), and finally digested and ligated into pBluescript KS+. The strategy used for the construction of plasmids carrying ribozymes with modified substrate recognition domains is described in the Results. All constructs were verified by DNA sequencing.

RNA synthesis

In vitro transcription. HDAg mRNA was transcribed from *Hin*dIII-linearized pKSAgS, while ribozymes were transcribed from *Sma*I-linearized ribozyme encoding plasmids. *In vitro* transcriptions were performed with T7 RNA polymerase with or without 50 μCi [α-^{32}P]GTP (Amersham) under conditions described previously (10). The mRNA and ribozyme products were purified on denaturing 4 and 15% polyacrylamide gels (PAGE, 19:1 ratio of acrylamide to bisacrylamide), respectively, containing 1× TBE and 7 M urea. Products were visualized either by autoradiography or UV shadowing. Bands were cut out and eluted overnight at 4°C in 0.5 M ammonium acetate, 0.1% SDS solution. Transcripts were then ethanol precipitated, washed, dried and the quantity determined by either spectrophotometry at 260 nm or ^{32}P counting.

Small substrate synthesis. Small substrates (11 nt) were syn-thesized either by *in vitro* transcription from templates formed by two annealed oligonucleotides as described previously (10), or chemically on an automated oligonucleotide synthesizer (Keck Biotechnology Resource Laboratory, Yale University) and then deprotected according to a procedure reported previously (11). Substrates were purified on 20% denaturing PAGE gels as described above.

Oligonucleotide probing

DNA oligonucleotides complementary to the potential target sites were purchased from Gibco-BRL and 5′-end labeled using T4 polynucleotide kinase (Pharmacia) in the presence of 10 μCi [γ-^{32}P]ATP. Labeled oligonucleotides (~2500 c.p.m.; ~0.05 nM) and unlabeled mRNA (2.4–1200 nM) were hybridized together for 10 min at 25°C in a solution containing 50 mM Tris–HCl

pH 7.5 and 10 mM MgCl$_2$ in a final volume of 15 μl. Loading solution (2 μl of 1× TBE, 10 mM MgCl$_2$, 40% glycerol, 0.25% bromophenol blue and 0.25% xylene cyanol) was added, and the resulting solutions fractionated on native 5% PAGE gels (30:1 ratio of acrylamide to bisacrylamide, 50 mM Tris-borate pH 8.3, 10 mM MgCl$_2$ and 5% glycerol) at 4°C in the presence of recirculating 50 mM Tris-borate pH 8.3 and 10 mM MgCl$_2$ buffer. The dried gels were analyzed with the aid of a PhosphorImager (Molecular Dynamics). RNase H probing was performed using the same oligonucleotides. In these experiments randomly labeled S-HDAg mRNA (~10 000 c.p.m.; ~10 nM) and unlabeled oligonucleotides (1 μM) were annealed as described for gel shift assays for 10 min, then 0.2 U of *Escherichia coli* RNase H (Pharmacia) was added and the reaction incubated at 37°C for 20 min. The reactions were stopped by the addition of stop solution (3 μl of 97% formamide, 10 mM EDTA, 0.25% bromophenol blue and 0.25% xylene cyanol), fractionated on 5% denaturing PAGE gels and analyzed by autoradiography.

In vitro cleavage assays and kinetic analyses

Cleavage assays were performed at 37°C under single turnover conditions with either randomly labeled mRNA (~10 nM) or 5′-end labeled small substrates (<1 nM), and an excess of ribozyme (2.5 μM) in 10 μl final volume containing 50 mM Tris–HCl pH 8.0 and 10 mM MgCl$_2$. A pre-incubation of 5 min at 37°C preceded the addition of the Tris–magnesium buffer which initiates the reaction. After an incubation of 1–3 h at 37°C, stop solution (5 μl) was added and the mixture quickly stored at –20°C until its fractionation on 5% denaturing PAGE gels and subsequently autoradiography. Cleavage sites of the active ribozymes were verified by primer extension assays as described previously (12). Briefly, oligonucleotides were synthesized to have complementary sequence to positions downstream (~100 positions) from the cleavage site according to the mRNA. For example for the cleavage site of Rz-12, the oligonucleotide primer, 5′-CTTTGATGTTCCCCAGCCAGG-3′ (21mer), was used in the reverse transcriptase reaction containing the ribozyme cleavage reaction mixture.

Active ribozymes (Rz-1, -11 and -12) were characterized under single turnover conditions essentially as described previously (10,13). Briefly, either randomly labeled mRNA (20 or 40 nM), or trace amounts of the corresponding 5′-end labeled small model RNA substrate (11 nt; <1 nM), were mixed with various amounts of unlabeled ribozyme (0.5–10 μM for mRNA; 5–250 nM for small substrates), and the volume adjusted to 18 μl with H$_2$O. The mixtures were pre-incubated for 5 min at 37°C prior to reaction initiation as described above. Aliquots (2 μl) were periodically removed, added to stop solution (5 μl), quickly frozen and analyzed by 5% (mRNA) or 20% (small substrate) denaturing PAGE gels. Substrate and product bands were quantified with a PhosphorImager (Molecular Dynamics). Rate constants (k$_{obs}$) were determined and kinetic parameters estimated (k$_{cat}$ and K$_{M'}$) as described previously (10,12). The maximal cleavage (i.e. end-point) of 250 nM of small substrates were similarly determined with several other ribozymes. Finally, Rz-12 was studied under multiple turnover conditions. Briefly, an excess of unlabeled mRNA (25–1000 nM) and randomly labeled mRNA (20 nM) were incubated with a constant concentration of ribozyme (20 nM). The conditions were similar to those described above with the exception that initial velocities were determined

using the linear proportion of the cleavage curves, and k_{cat} and K_M were calculated by standard Lineweaver–Burk plots.

RESULTS

Selection of potential target sequences in HDAg mRNA

Since the targeting of HDAg mRNA is of clinical interest, we selected several regions present in most of the HDV variants. We aligned all complete HDV variants and partial HDAg mRNA sequences reported as of January 1, 1997 (17 complete and 35 partial sequences) using the ClustalW package (8). In our search for potential delta ribozyme target sequences in HDAg mRNA, we used two rules: (i) a potential target sequence should be perfectly conserved in >80% of the HDV variants; and (ii) the conserved sequences should harbor the consensus recognition sequence of a delta ribozyme (i.e. YGN_6). Ten potential target sites were found within the HDAg mRNA (numbered from 1 to 10; see Table 1). In order to maximize our chances of developing efficient ribozymes, we selected two additional sites which were observed to be highly accessible (numbered 11 and 12; see Table 1) according to nuclease probing assays (G.Roy and J.P.Perreault, unpublished data). These two sites harbor the consensus recognition sequence (e.g. YGN_6), but were conserved between the HDV sequence variants at slightly <80% and therefore were not found previously.

Table 1. Summary of the mRNA structure probing

Site	Position in the mRNA	mRNA sequence	Binding shift assays (K_d in nM)	RNase H assays
1	181-188	UGGCUGGG	+++ (69)	+++
2	245-253	CGAAGAGG	-	+
3	318-325	CGACAAGG	-	+
4	356-365	CGAGAACA	+ (663)	+
5	485-492	UGUGAACC	-	+
6	487-494	UGAACCCC	-	-
7	508-515	CGAGGGGA	+++ (62)	+++[a]
8	527-534	CGGCUUCG	-	-
9	556-563	CGGAGUCC	++ (92)	++
10	663-670	UGUCGACC	-	-
11	45-52	CGAGUCGA	+++ (59)	++
12	90-97	UGGGUGGC	+++ (49)	+++

The minus sign (–) indicates that a site could not be probed while the plus signs represent the efficiency of either oligonucleotide binding or RNase H products produced (more plus signs equals greater efficiency). K_d is dissociation constant.
[a]Non-specific cleavage products were observed.

Ribozyme target sequences located in single-stranded regions of an mRNA have a higher potential as target sites because they should be more accessible to ribozyme attack than those found in double-stranded regions. Within the double-stranded regions the ribozyme might compete unfavorably with intramolecular base-pairing in order to bind its substrate (14,15). Consequently, we aimed to evaluate the accessibility of the various selected sites of the mRNA used in the present work (Table 2). This RNA species, which is synthesized by *in vitro* transcription from the pKSAgS plasmid (Materials and Methods), included an HDAg mRNA sequence (an HDV genotype I) plus 5′-end sequences from the vector (positions –83 to –52). However, the additional sequences did not significantly alter the predicted secondary structure as compared to the HDV sequence alone (data not shown).

In order to specifically probe all sites, we performed both binding shift assays and ribonuclease H (RNase H) hydrolysis

Table 2. Synthesized delta ribozymes

```
Ribozyme    P1 stem sequence        Size of expected cleavage products (nt)
Rz-1        CCCAGCU                 265 ,  551
Rz-2        CCUCUUU                 330 ,  486
Rz-3        CCUUGUU                 403 ,  413
Rz-4        UGUUCUU                 440 ,  376
Rz-6        GGGGUUU                 572 ,  244
Rz-7        UCCCCUU                 593 ,  223
Rz-9        GGACUCU                 640 ,  176
Rz-11       UCGACUU                 130 ,  686
Rz-12       GCCACCU                 175 ,  641

mRNA sequence

1    CACCGCGGUG GCGGCCGCUC UAGAACUAGU GGAUCCCUCG GGCUCGGGCG GCGAGUCCAG
61   CAGUCUCCUC UUUACAGAUA AUGUAAGAGU ACUGAGGACU GCCGCCUCUA GCCGAGAUGA
121  GCCGGUCCGA GUCGAGGAAG AACCGCGGAG GGAGAGAAGA GAUCCUCGAG CAGUGGGUGG (11,12)
181  CCGGAAGAAA GAAGUUAGAG GAACUCGAGA GAGACCUCCG GAAGACAAAG AAGAAACUCA
241  AGAAGAUAGA GGACGAAAAU CCCUGGCUGG GGAACAUCAA AGGAAUUCUC GGAAAGAAGG (1)
301  AUAAGGAUGG AGAGGGGGCU CCCCCCGCGA AGAGGGCCCG AACGGACCAG AUGGAGGUAG (2)
361  ACUCCGGACC UCGGAAGAGG CCUCUCAGGG GAGGAUUCAC CGACAAGGAG AGGCAGGAUC (3)
421  CCGACGAAGG AAGGCCCUCG AGAACAAGAA GAAGCAGCUA UCGGCGGGAG GCAAGAACCU (4)
481  CAGCAAGGAG GAAGAAGAGG AACUCAGGAG GUUGACCGAG GAAGACGAGA GAAGGGAAAG
541  AAGAGUAGCC GGCCCGCCGG UUGGGGGUGU GAACCCCCUC GAAGGUGGAU CGAGGGGAGC (6,7)
601  GCCCGGGGGC GGCUUCGUCC CCAAUCUGCA GGGAGUCCCG GAGUCCCCCU UCUCUCGGAC (9)
661  CGGGGAGGGG CUGGACAUCA GGGGAAACCA GGGAUUUCCA UAGGAUAUAC UCUUCCCAGC
721  CGAUCCGCCC UUUUCUCCCC AGAGUUGUGC ACCCCAGUGA AUAAAGCGGG UUUCCACUCA
781  CAGGGUUUGCG UCUCGCGUCC UUCUUUCCUC UUC
```

Upper part is the ribozyme nomenclature with the sequence composing the P1 stem domain and the size of the expected products. Lower part is the mRNA sequence. The mRNA sequences targeted by ribozymes are underlined, and the ribozyme number is in parentheses on the right.

using 8mer oligonucleotides of sequence corresponding to the recognition domain of the ribozyme (i.e. N_6TG). We assumed that the hybridization of an oligonucleotide to the mRNA is an indication of the accessiblity of the site. In the binding shift assay, the oligonucleotides were 5′-end labeled, preincubated with unlabeled mRNA and the resulting mixtures fractionated on native gels (Fig. 2A). Both the free and bound oligonucleotide fractions were quantified, binding curves drawn and equilibrium dissociation constants (K_d) estimated (see Fig. 2B for an example, and Table 1 for the compiled results). Six oligonucleotides (sites 2, 3, 5, 6, 8 and 10) did not result in a band shift, even with an mRNA concentration of 1.2 µM, suggesting that these sites are relatively inaccessible. In contrast, five oligonucleotides had a relatively high affinity for the mRNA (sites 1, 7, 9, 11 and 12; K_d ~60 nM), and one had a moderate affinity (site 4; K_d of 663 nM).

Ribonuclease H, which specifically cleaves the RNA of a DNA–RNA duplex, can be used to verify whether or not the oligonucleotide binding is specific to a target sequence. Randomly labeled mRNA was preincubated with unlabeled oligonucleotides, hydrolyzed by RNase H, and the mixtures resolved on denaturing gels (see Fig. 2C for an example, and Table 1 for the compiled results). The presence of the oligonucleotides corresponding to sites 6, 8 and 10 did not produce RNase H hydrolysis products, confirming the inaccessibility of these three sites. In the presence of oligonucleotides corresponding to sites 1, 2, 3, 4, 5, 9, 11 and 12, products of appropriate size were observed. In contrast, the oligonucleotide corrresponding to site 7 gave several non-specific products, suggesting that it bound the mRNA at more than one position (Fig. 2C). This result may be explained by the fact that *E.coli* RNase H requires only 4 bp of heteroduplex for its activity (16). Thus, with the exception of site 7, the RNase H results confirm the specificity of the binding shift assays.

Ribozyme cleavage of the mRNA

The delta ribozyme used in this work, which corresponds to the antigenomic version, was previously characterized for its ability to cleave small model substrates (Fig. 1). This ribozyme is synthesized by *in vitro* transcription from a T7 RNA promoter
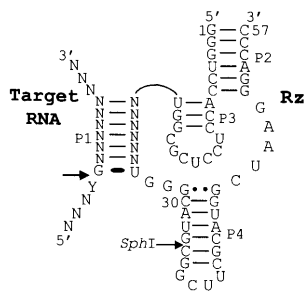
Figure 1. Sequence and proposed secondary structure of the delta ribozyme used. The illustated secondary structure is that predicted by the pseudoknot model which includes four stems (P1–P4; ref. 17). The modifications of the wild-type sequence to produce the delta ribozyme used in this work were described previously (10,16). The minimal P1 stem requirements for both the ribozyme and substrate strands are shown; Y and N represent a pyrimidine and any nucleotide (G,A,U,C), respectively. In the target RNA substrate the arrow points to the cleavage site. In the ribozyme (Rz), the homopurine basepair at the top of the P4 stem is represented by two dots (G··G), while the arrow indicates the *Sph*I restriction site used for modification of the ribozyme binding sequence.

immediately followed by a minigene cloned into pUC19 vector. The minigene was designed so as to have unique *Sal*I and *Sph*I restriction sites which permit modification of the recognition domain of the ribozyme (i.e. the 7 nt of the P1 stem; ref. 17). Specifically, the *Sal*I site is located slightly upstream of the T7 RNA promoter, while the *Sph*I site is located in the P4 stem of the ribozyme (Fig. 1). Therefore, the DNA insert between these two restriction sites constitutes an exchangeable cassette permitting construction of the nine clones encoding ribozymes with sequences required to recognize the selected sites (Table 2). The selection of the target sites was performed according to the structural data: sites 1, 9, 11 and 12 appeared to be accessible by both structure probing methods, while sites 2, 3, 4 and 7 appeared to be accessible by at least one biochemical approach (Table 1). Therefore, we constructed the plasmid containing the chosen ribozyme sequences for all of these sites. Among the relatively inaccessible sites (i.e. sites 5, 6 and 10), only site 6 was considered (as a negative control).

The ability of each ribozyme to cleave the labeled mRNA was tested under pre-steady-state conditions ([Rz]>[S]) in which a 250-fold excess of ribozyme was individually mixed with random-labeled mRNA, preincubated at 37°C, and the reaction initiated by the addition of MgCl2 to a final concentration of 10 mM. After 3 h of incubation at 37°C, the reactions were quenched and analyzed on polyacrylamide gels (Fig. 3A). Among the nine constructed ribozymes, cleavage products were detected only in the assays catalyzed by Rz-1, -11 and -12. Even then Rz-11 required an over-exposure of the gel in order to confirm the presence of the cleavage products. In order to enhance the ribozyme–substrate binding, heat-denaturation (65°C for 2 min), coupled to snap-cooling on ice (2 min), was performed prior to the 37°C preincubation (data not shown). Under these conditions, as well as in the presence of a crude cytoplasmic protein extract from Hep-G2 cells, again only Rz-1, -11 and -12 exhibit catalytic activity (data not shown). These results indicate that the six other ribozymes (Rz-2, -3, -4, -6, -7 and -9) were inactive because either they did not bind the mRNA, or they did not cleave the mRNA subsequent to formation of the ribozyme–substrate complex (see below).
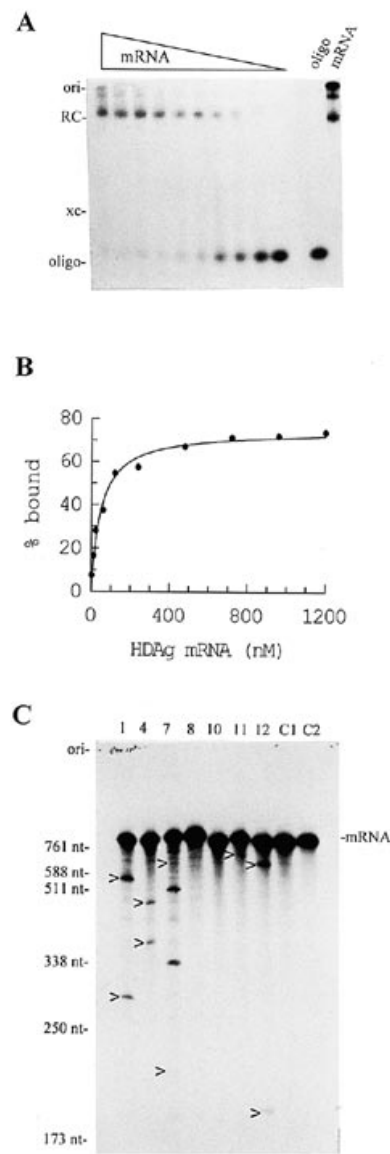

Figure 2. Messenger RNA probing with oligonucleotides. (**A**) Autoradiogram of a gel shift assay for site 1. 5′-end labeled DNA oligonucleotide was incubated with 10 decreasing mRNA concentrations, ranging from 1200 to 2.4 nM, prior to fractionation on a native gel. Lanes labeled oligo and mRNA are the 5′-end labeled oligonucleotide alone and the randomly labeled mRNA alone, respectively. The position of migration of the retarded complex (RC), oligonucleotide (oligo), xylene cyanol (xc) and the origin (ori) are indicated. (**B**) Plot of the bound oligonucleotide corresponding to site 1 as a function of mRNA concentration. (**C**) Autoradiogram of an RNase H assay for various sites. The number at the top of a lane indicates the number of the site probed, with the exceptions of C1 and C2 which indicate that the mRNA was incubated either in the presence or the absence of RNase H, respectively. On the left of the gel the positions of the RNA molecular weight markers are indicated.

The ability of the three active ribozymes to cleave the mRNA was further characterized under pre-steady-state conditions ([Rz]>>[S]) using various concentrations of ribozyme. Briefly, increasing concentrations of these individual ribozymes (i.e. Rz-1, -11 and -12) allowed the detection of larger concentration of products. Examples of a time course experiment with Rz-11

(10 µM) and Rz-12 (5 µM) are shown in Figure 3B and C. Rz-12 appeared to be the most efficient ribozyme against HDAg mRNA. The sizes of the products produced by the three active ribozymes correspond to those expected for their predicted cleavage sites (Table 2). RNase H hydrolysis and ribozyme cleavage mixtures for Rz-1, -11 and -12 were migrated side-by-side onto denaturing PAGE, and reaction products exhibited corresponding electrophoretic mobility, suggesting that the ribozymes cleaved at the expected positions. In order to confirm the cleavage specificity of the active ribozymes, primer extension assays were performed with the cleavage reaction mixtures. For example, for the cleavage site of Rz-12, the 5′ end of the 3′ cleavage product corresponds to the expected position (Fig. 4, arrow), therefore confirming that Rz-12 targeted to the accurate site.

Cleavage of small substrates

In order to learn more about the efficiency of both the active and inactive ribozymes, we synthesized small model substrates with sequences corresponding to some sites on the mRNA (Table 3). Cleavage of the 11 nt long substrate yielded 5′ and 3′ products of 4 and 7 nt, respectively. Trace amounts of end-labeled substrates (<1 nM) were incubated in the presence of an excess of ribozyme (250 nM), and the maximal cleavage percentages (end-point) determined as a comparative parameter. The observed maximal cleavage percents varied significantly between the different ribozymes (Table 3), suggesting that the sequence of both the substrate and the binding domain (stem P1) of the ribozyme influence cleavage activity.

Table 3. Cleavage of small substrates

Ribozyme	Substrate	End-point % cleavage
Rz-1	5' CCCU ↓ GGCUGGG 3'	<1
	<u>GGGC</u> ↓ GGCUGGG	79
	<u>GGGU</u> ↓ GGCUGGG	11
Rz-2	CCGC ↓ GAAGAGG	<1
	C<u>G</u>GC ↓ GAAGAGG	1
	<u>GGG</u>C ↓ GAAGAGG	1
Rz-3	CACC ↓ GACAAGG	4
	<u>GGG</u>C ↓ GACAAGG	60
Rz-4	CCUC ↓ GAGAACA	1
	<u>GGG</u>C ↓ GAGAACA	50
Rz-6	GUGU ↓ GAACCCC	21
	GG<u>G</u>U ↓ GAACCCC	4
Rz-7	GAUC ↓ GAGGGGA	24
Rz-9	UCCC ↓ GGAGUCC	<1
	<u>GGG</u>C ↓ GGAGUCC	<1
Rz-11	GUCC ↓ GAGUCGA	3
	<u>GGG</u>C ↓ GAGUCGA	55
Rz-12	CAGU ↓ GGGUGGC	11
	C<u>C</u>GU ↓ GGGUGGC	6
	C<u>CC</u>U ↓ GGGUGGC	2
	<u>GG</u>GU ↓ GGGUGGC	44

The values were calculated from at least two independent experiments. Underlined nucleotides correspond to mutated position(s) compared to the mRNA sequences, while arrows indicate cleavage sites.

Surprisingly, Rz-1 did not cleave its wild-type small substrate, but cleaved the similar sequence within the mRNA (see above). The substrate's 5′ portion, which corresponds to positions –4 to
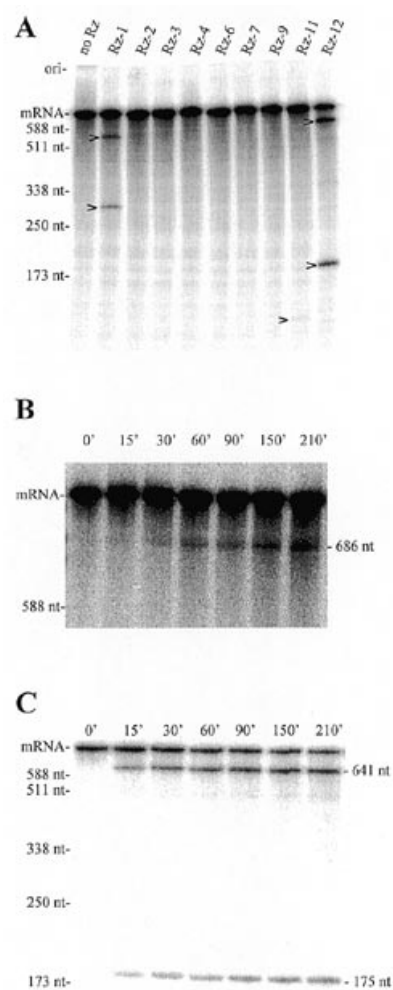

Figure 3. Cleavage of the mRNA by delta ribozymes. (**A**) Autoradiogram of mRNA cleavage assays with all ribozymes. Randomly labeled mRNA was incubated with a 250-fold excess of ribozyme for 3 h at 37°C (Materials and Methods). The cleavage products of Rz-1, -11 and -12 are indicated. Ori indicates origin of migration. (**B**) and (**C**) Autoradiograms of time course experiments for Rz-11 (10 µM) and Rz-12 (5 µM), respectively, under pre-steady-state conditions in the presence of 40 nM substrate. The time points in minutes are indicated at the top of each lane. See Materials and Methods for detailed procedures. The RNA molecular weight markers are indicated on the left of the gel, and the size of the products are on the right. For Rz-11 (B) long migration was required to separate the longer product (686 nt) from the substrate, as a consequence the shorter product ran out of the gel.

–1 upstream to the cleavage site, harbors the sequence 'CCCU'. We suspect that these cytosines (positions –4 to –2) can basepair with the opposite guanosines (positions 27–29) linking the P1 and P4 stems of the ribozyme (i.e J1/4 junction, Fig. 1). If these basepairs are indeed formed, most likely the ribozyme–substrate complex folds into an inactive conformation. Perhaps these additional basepairs cannot be formed with the mRNA because the cytosines are already involved in a double-stranded region of the molecule, and the ribozyme is consequently active. In order to verify this hypothesis, mutant substrates with either 'GGGC' or 'GGGU' 5′ end sequences were synthesized. These substrates were cleaved more efficiently by Rz-1, although at a different level showing a preference for a C as compared to U at position
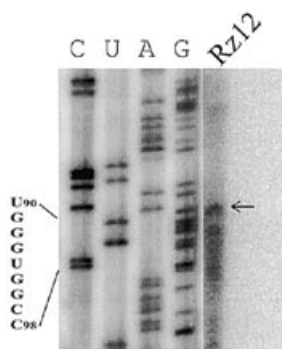
Figure 4. Verification of the Rz-12 cleavage site. The Rz-12 cleavage reaction mixture (i.e. containing 120 nM mRNA and 700 nM Rz-12), was recovered after a 1 h incubation, and RNA used as templates for reverse transcriptase reaction. The reverse transcriptase products were migrated along the sequencing ladder which was performed using the same primer. The position of the cDNA product (i.e. the cleavage site) is indicated by the arrow. The sequence downstream of the cleavage site is shown on the left.

–1 (Table 3). Similar mutant substrates were produced for several ribozymes and yielded identical results with the exception of Rz-2 and -9 (see below). Higher guanosine residue content in the 5′ end portion (i.e. positions –4 to –2) allows for more efficient cleavage as compared to the wild-type sequence which includes either C or U (Table 3). In contrast, we synthesized mutant substrates for Rz-12 in which a wild-type substrate harboring a 'CAGU' 5′ end was the most efficiently cleaved molecule. Both one and two cytosines were introduced in positions –3 or –2 and –3, respectively. The introduction of these cytosines yielded reduced values of cleavage end-points, notably so with the addition of the second cytosine. When the 'CA' (position –4,–3) was replaced by 'GG', the cleavage activity was better than that of the wild-type substrate.

Both the Rz-2 and -9 inefficiently cleaved (<1%) both their wild-type substrates and G-rich mutant substrates (Table 3). These substrates share the characteristic of having a G at position +4 after the cleavage site. A recent study of the effect of alterations in the P1 stem on the kinetic and thermodynamic characteristics of delta ribozyme cleavage demonstrated that a G at position +4 of the substrate yielded inefficient cleavage, while the presence of any other base (i.e. A, C or U) allowed cleavage to occur, albeit at different levels (S.Ananvoranich, D.Lafontaine and J.P.Perreault, unpublished data). This conclusion is in agreement with the results obtained with the various substrates. When a G is at position +4, the cleavage activity was limited to ≤1%, while with an A, C or U at this position the maximal cleavage level was attained.

DISCUSSION

Delta ribozyme cleavage of an mRNA

In order to verify whether or not delta ribozyme can catalyze the cleavage of an mRNA *in trans*, we have engineered delta ribozymes that specifically recognize and subsequently cleave a derivative of the HDAg mRNA. Initially, we identified the most likely sequences of the mRNA used using binding shift assays and RNase H hydrolysis (Table 1). Three out of the four sites (i.e. Rz-1, -11 and -12) for which consistent indications that the

binding sites were located within single-stranded regions were obtained, were cleaved by ribozymes. While all other sites that appeared not relatively accessible by either one or two approaches cannot be cleaved. These results confirm the importance of studying the structure of the target mRNA prior to the design of a ribozyme. More importantly, these results show that delta ribozyme can catalyze the cleavage of a natural mRNA *in trans*, at least *in vitro*. This is an original demonstration with delta ribozyme.

The most active ribozyme (Rz-12) was characterized under steady-state conditions ([S]>>[Rz]; data not shown). Under the conditions used, Rz-12 has a Michaelis–Menten constant (K_M) of 550 nM for the mRNA, which is comparable to that estimated for the cleavage of a small substrate (11 nt) by an almost identical delta ribozyme (i.e. 510 nM; ref. 18). However, the catalytic rate constant ($k_{cat} = 0.012$ min^{-1}) of Rz-12 for mRNA cleavage was 50-fold slower than that for the cleavage of the small substrate by the almost identical ribozyme (i.e. k_{cat} of 0.65 min^{-1}). These results suggest that the binding process is similar for both the small (11 nt) and larger (mRNA) substrates, but that the cleavage step occurs more slowly with the mRNA under steady-state conditions. At the highest mRNA concentration tested (1000 nM), more than six turnovers were observed within the considered linear portion of the curve. In other words, several mRNA molecules can be cleaved successively. This is an essential property for the further development of efficient ribozyme-based gene therapy. Rz-12 was also investigated under pre-steady-state conditions ([Rz]>>[S], data not shown). The mRNA cleavage gave k_{cat} and apparent K_M of 0.03 min^{-1} and 0.8 µM, respectively, compared to 0.94 min^{-1} and 12 nM for the small substrates. Single turnover results show that a larger concentration of mRNA (~70-fold) as compared to the small substrate is required to saturate the ribozyme. However, even saturated ribozymes remained 30-fold slower in their cleavage of the mRNA as compared to that of the small substrates.

Substrate specificity of delta ribozyme

The compiled results for the cleavage of the small substrates established a purine preference in positions –4, –3 and –2. Unlike pyrimidines, these purines probably do not have the ability to basepair with the guanosines of the J1/4 junction. The formation of these basepairs may result in the folding of the RzS complex into an inactive structure. However, the purine rule in positions –4 to –2 is not absolute, since at least two circumstances exist in which the presence of a pyrimidine in any position between –4 and –2 can be tolerated without ribozyme inactivation. Specifically, the presence of a pyrimidine in these positions is acceptable if these nucleotides are involved in a double-stranded structure with another region of the mRNA, as is proposed for site 1 within the the full-length mRNA; or if the two pyrimidines are not consecutive. Most likely the presence of only one basepair is insufficient to stabilize the inactive structure (e.g. Rz-12). It seems that positions –2, –3 and –4 can be changed to a pyrimidine if it is not followed by a second pyrimidine. Therefore, considering the requirement for a guanosine immediately after the cleavage site for formation of a wobble basepair, and the six to seven consecutive basepairs forming the P1 stem (2), we may summarize the substrate specificity as the following:

$$(R)_{-4} (R)_{-3} (R)_{-2} Y_{-1} \downarrow G_1 N_2 N_3 (A/C/U)_4 N_5 N_6 N_7$$

where R and Y indicate purine and pyrimidine, N is for any nucleotide that can basepair with the ribozyme, and the parentheses indicate that the nucleotide in question is not exclusively restricted to being a purine (see above). The P1 domain is composed of the nucleotides that basepair with the ribozyme; hence, these nucleotides can be defined as internal determinants of substrate specificity. Several investigations have been performed addressing the questions related to the P1 domain specificity. It has been demonstrated that cleavage activity was not destroyed by the interchange of between one and four nucleotide pairs between the substrate and the ribozyme (19–22). However, we have recently shown a clear preference for C, U or A at position +4 of the substrate in order for cleavage to occur (10). In contrast, the nucleotides upstream of the cleavage site should not basepair with the ribozyme (i.e positions –4 to –1). These nucleotides do not directly contribute to substrate recognition (e.g. substrate binding); however, they do play a role in 'proofreading' as they can allow folding into either an active or inactive structure. Indeed, the identity of these nucleotides is essential for efficient cleavage, therefore they contribute to substrate specificity, likely as external determinants.

CONCLUSION

In this report we demonstrate the ability of delta ribozyme to catalyze, *in trans*, the specific cleavage of a full-length mRNA. Delta ribozyme offers the advantage of having the natural ability to function in the presence of human proteins; therefore, it can be considered as a suitable ribozyme for gene therapy development. Furthermore, the results presented here shed light on new features that contribute to the substrate specificity of delta ribozyme cleavage. This work clearly illustrates the potential of this ribozyme as a therapeutic tool.

ACKNOWLEDGEMENTS

REFERENCES

1 Lai,M.M.C. (1995) *Annu. Rev. Biochem.*, **64**, 259–286.
2 Been,M.D. and Wickham,G.S. (1997) *Eur. J. Biochem.*, **247**, 741–753.
3 Mercure,S., Lafontaine,D., Roy,G. and Perreault,J.-P. (1997) *Médecine/ Sciences*, **13**, 662–669.
4 Pattnaik,A.K., Ball,L.A, LeGrone,A.W. and Wertz,G.W. (1992) *Cell*, **69**, 1011–1020.
5 Chowrira,B.H., Pavco,P.A. and McSwiggen,J.A. (1994) *J. Biol. Chem.*, **269**, 25856–25864.
6 Perrotta,A.T. and Been,M.D. (1996) *Nucleic Acids Res.*, **24**, 1314–1321.
7 Lafontaine,D., Mercure,S. and Perreault,J.-P. (1997) *Nucleic Acids Res.*, **25**, 123–125.
8 Thompson,J.D., Higgins,D.G. and Gibson,T.J. (1994) *Nucleic Acids Res.*, **22**, 4673–4680.
9 Chao,M., Hsieh,S.Y. and Taylor,J. (1990) *J. Virol.*, **64**, 5066–5069.
10 Ananvoranich,S. and Perreault,J.-P. (1998) *J. Biol. Chem.*, **273**, 13182–13188.
11 Perreault,J.-P. and Altman,S. (1992) *J. Mol. Biol.*, **226**, 399–409.
12 Côté,F. and Perreault,J.-P. (1997) *J. Mol. Biol.*, **273**, 533–543.
13 Hertel,K.J., Herschlag,D. and Uhlenbeck,O.C. (1996) *EMBO J.*, **15**, 3751–3757.
14 Campbell,T.B. and Cech,T.R. (1995) *RNA*, **1**, 598–609.
15 Birikh,K.R., Berlin,Y.A., Soreq,H. and Eckstein,F. (1997) *RNA*, **3**, 429–437.
16 Hogrefe,H.H., Hogrefe,R.I., Walder,R.Y. and Walder,J.A. (1990) *J. Biol. Chem.*, **265**, 5561–5566.
17 Roy,G., Ananvoranich,S. and Perreault,J.-P. (1997) *Nucleic Acids Symp. Ser.*, **36**, 93–95.
18 Mercure,S., Lafontaine,D., Ananvoranich,S. and Perreault,J.-P. (1998) *Biochemistry*, **37**, 16975–16982.
19 Perrotta,A.T. and Been,M.D. (1991) *Nature*, **350**, 434–436.
20 Wu,H.N., Wang,Y.J., Hung,C.F., Lee,H.J. and Lai,M.C.C. (1992) *J. Mol. Biol.*, **223**, 233–245.
21 Been,M.D., Perrotta,A.T. and Rosenstein,S.P. (1992) *Biochemistry*, **31**, 11843–11852.
22 Perrotta,A.T. and Been,M.D. (1992) *Biochemistry*, **31**, 16–21.